ON THE EVOLUTION OF ANISOTROPIC ELASTIC PROPERTIES DURING METAL FORMING

A. BERTRAM and T. BÖHLKE

Institute of Mechanics, Otto-von-Guericke-University Magdeburg, Germany

Abstract

Since single crystalline copper exhibits a significant degree of elastic anisotropy, the polycrystalline elastic properties can be affected by the crystallographic texture in an amount that is relevant for engineering applications. In the present paper the evolution of the elastic properties is studied for different deformation paths.

Keywords: Finite Inelastic Deformations, Texture Induced Elastic Anisotropy

1. Introduction

There is a rapid progress in the capabilities to simulate the evolution of material properties due to macroscopic deformation or loading processes. The evolution of material properties is caused by microstructural changes, like localization phenomena or the formation of morphological and crystallographic textures.

The crystallographic texture evolution of materials with high and intermediate stacking fault energy (e.g. pure copper) can be determined by the Taylor model within a first-order accuracy (Leffers 1993). In the present paper the evolution of the elastic properties of polycrystalline copper undergoing large inelastic deformations is numerically studied for three finite deformation modes using the Taylor-Lin-model (Asaro and Needleman 1985).

The elastic law on the microscale, i.e. within the grains, is derived from the assumption that the elastic behaviour is not affected by inelastic deformations (Bertram 1999). The simulations are restricted to proportional deformation processes, and so, only isotropic hardening models (Harren et al. 1989, Meric et al. 1994) are considered. The hardening parameters are taken from the literature (Wu et al. 1996).

For a given grain orientation distribution there are different methods to determine the elastic properties of a heterogeneous linear elastic material (Kocks et al. 1998). Simple estimations are those suggested by Voigt (1928) and Reuss (1929). The first assumed a constant strain, the latter a constant stress field in the aggregate. Under these assumptions, the effective fourth-order elasticity tensors turn out to be volume averages of the corresponding local fields, and can be derived directly from texture data. The volume averages of the local elastic moduli generally result in

more or less anisotropic elasticity tensors if determined from empirical texture data. In order to determine effective properties in the isotropic case, the averaging has to be performed in the orientation space with a constant orientation distribution function. The advantage of these approaches, which represent arithmetic means of the local properties, is that they give bounds for the macroscopic strain energy density (Hill 1952).

Therefore, alternative approaches have been developed in order to obtain more precise information from the texture data. Hill (1952) proposed both an arithmetic and a geometric mean of the isotropic bounds of Voigt and Reuss, which give estimations closer to experimental values. An approach that focusses on an homogenization that guarantees unique effective properties, such that the inverse of the mean compliance is equal to the mean stiffness, was given by Aleksandrov and Aizenberg (1967) and further developed by Matthies and Humbert (1995). Within that approach the geometric mean of the local elastic moduli is used. Beside the uniqueness, the advantage of this method lies in improved predictions of experimental values. The disadvantage is that the physical implications are unclear since any assumption concerning the kinematic or dynamic fields is avoided.

On the macroscopic scale material symmetries determined by experiments or simulations generally exist only in some approximate sense, because the microstructure induces deviations from the behaviour described by classical point-groups. For metals the elastic behaviour can be linearized within elastic ranges. Therefore, a fourth-order tensor is sufficient for the description of the mechanical properties within some elastic range. In order to identify the anisotropy, the fourth-order elasticity tensor given by the homogenization technique can be approximated by fourth-order tensors corresponding to distinct symmetry groups. In this paper an approximation is suggested, which contains the isotropic bounds as special cases if applied to the isotropic bounds by Voigt and Reuss, and which is furthermore applicable to any fourth-order elasticity tensor given by experiments or simulations.

The texture induced elastic anisotropy is investigated by simulating a plane strain compression, a drawing, and a simple shear deformation. The evolving macroscopic elastic properties due to the texture development are approximated by linear elastic laws with the ten traditional, distinct symmetries.

2. Single crystal and polycrystal elasticity

It is assumed that the symmetric stress tensor $\mathbf{T}$ is given as a linear invertible map of the symmetric strain tensor $\mathbf{E}$. The operators of this map - the fourth-order stiffness C and compliance tensor S - are specified by the symmetry group $\mathcal{S}$ of the material being a subgroup of the orthogonal group

$$\mathbf{T} = \mathsf{C}[\mathbf{E}], \qquad \mathbf{E} = \mathsf{S}[\mathbf{T}], \qquad \mathbf{H}^{\mathrm{T}}\mathsf{C}[\mathbf{E}]\mathbf{H} = \mathsf{C}[\mathbf{H}^{\mathrm{T}}\mathbf{E}\mathbf{H}], \qquad \forall\, \mathbf{H} \in \mathcal{S}. \tag{1}$$

The elasticity tensors are positive definite and possess the major symmetry in the case of hyperelastic materials. Without loss of generality, the symmetry in the first and last pair of indices is assumed.

Voigt's and Reuss' assumption of constant strain and stress fields, respectively, yield the most simple estimations of the elastic properties of the aggregate. The macroscopic elasticity tensors are then given by the volume averages of the corre-

sponding local fields

$$\mathbf{C}^V = \frac{1}{V}\int_V \mathbf{C}\,\mathrm{d}V, \qquad \mathbf{S}^R = \frac{1}{V}\int_V \mathbf{S}\,\mathrm{d}V \neq \mathbf{C}^{V-1}. \tag{2}$$

An approach that guarantees unique effective properties is given by the geometric mean (Aleksandrov and Aizenberg 1967, Matthies and Humbert 1995)

$$\mathbf{C}^A = \exp\left(\frac{1}{V}\int_V \ln(\mathbf{C})\,\mathrm{d}V\right), \qquad \mathbf{S}^A = \exp\left(\frac{1}{V}\int_V \ln(\mathbf{S})\,\mathrm{d}V\right) \equiv \mathbf{C}^{A-1}. \tag{3}$$

An estimation of the elastic properties with the additional assumption of a uniform orientation distribution follows by transforming the integrals (2) and (3) to the orientation space using $\mathrm{d}V/V = f(g)\,\mathrm{d}g$ and setting the orientation distribution function $f(g)$ equal to one (Bunge 1993)

$$\mathbf{C}^{VI} = \int_g \mathbf{C}(g)\,\mathrm{d}g, \qquad \mathbf{S}^{RI} = \int_g \mathbf{S}(g)\,\mathrm{d}g, \qquad \mathbf{C}^{AI} = \exp\left(\int_g \ln(\mathbf{C}(g))\,\mathrm{d}g\right). \tag{4}$$

If the orientation space is parameterized by Euler angles, the corresponding volume element is given by $\mathrm{d}g = \sin(\Phi)\,\mathrm{d}\Phi\,\mathrm{d}\varphi_1\,\mathrm{d}\varphi_2/8\pi^2$.

In the case of cubic single crystals the difference of the anisotropic and isotropic averages can be brought into the comprehensive form (Böhlke and Bertram 1999)

$$\mathbf{C}^V - \mathbf{C}^{VI} = f^V\mathbf{D}, \qquad \mathbf{S}^R - \mathbf{S}^{RI} = f^R\mathbf{D}, \qquad \ln(\mathbf{C}^A) - \ln(\mathbf{C}^{AI}) = f^A\mathbf{D}, \tag{5}$$

with

$$\mathbf{D} = \frac{\sqrt{30}}{30}\left(\mathbf{I}\otimes\mathbf{I} + 2\mathbf{I}^S - \frac{5}{V}\int_V \mathbf{A}\,\mathrm{d}V\right), \qquad \mathbf{A} = \sum_{i=1}^{3} \mathbf{g}_i\otimes\mathbf{g}_i\otimes\mathbf{g}_i\otimes\mathbf{g}_i, \tag{6}$$

$\mathbf{g}_i$ being the lattice vectors. $\mathbf{I}$ denotes the second-order identity tensor and $\mathbf{I}^S$ the identity on symmetric second-order tensors. The scalar factors in equations $(5)_{1,2,3}$ are given by

$$\begin{aligned} f^V &= \|\,\mathbf{C} - \mathbf{C}^{VI}\,\| &&\equiv \sqrt{30/25}\,|\,\lambda_3 - \lambda_2\,|\,,\\ f^R &= \|\,\mathbf{S} - \mathbf{S}^{RI}\,\| &&\equiv \sqrt{30/25}\,|\,1/\lambda_3 - 1/\lambda_2\,|\,,\\ f^A &= \|\,\ln(\mathbf{C}) - \ln(\mathbf{C}^{AI})\,\| &&\equiv |\ln(\lambda_3) - \ln(\lambda_2)\,|\,. \end{aligned} \tag{7}$$

The difference of the averages is influenced on the one hand by the degree of anisotropy of the single crystals through, e.g., $\|\,\mathbf{C} - \mathbf{C}^{VI}\,\|$, and on the other hand by the orientation distribution in form of the tensor $\mathbf{D}$. The norm $\|\,\mathbf{D}\,\|$ is equal to one for a single orientation, equal to zero for a uniform orientation distribution, and in the interval $(0,1)$ otherwise.

4. Numerical example

In this paper the texture induced elastic anisotropy is investigated by simulating a plane strain compression (A), a drawing (B), and a simple shear deformation (C). The corresponding deformation gradients are given by

$$\begin{aligned} A:&\quad \mathbf{F} = \kappa\mathbf{e}_1\otimes\mathbf{e}_1 + \kappa^{-1}\mathbf{e}_2\otimes\mathbf{e}_2 + \mathbf{e}_3\otimes\mathbf{e}_3, && \kappa \in [1,10],\\ B:&\quad \mathbf{F} = \kappa\mathbf{e}_1\otimes\mathbf{e}_1 + \kappa^{-1/2}\left(\mathbf{e}_2\otimes\mathbf{e}_2 + \mathbf{e}_3\otimes\mathbf{e}_3\right), && \kappa \in [1,10],\\ C:&\quad \mathbf{F} = \mathbf{I} + \kappa\mathbf{e}_1\otimes\mathbf{e}_2, && \kappa \in [0,5]. \end{aligned} \tag{8}$$

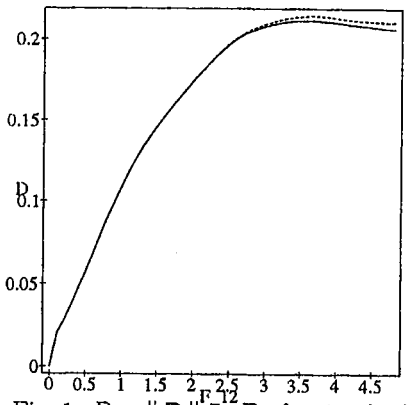

Fig. 1: $D = \| \mathbf{D} \|$ vs F_{12} for simple shear and different hardening laws, H1: (-), H2: (--).

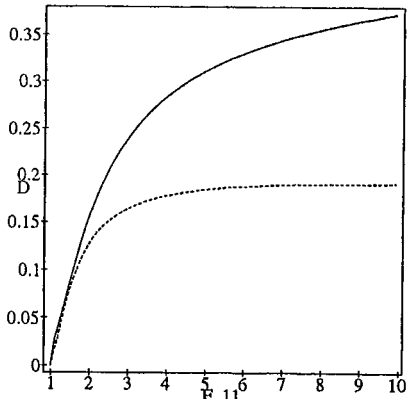

Fig. 2: $D = \| \mathbf{D} \|$ vs F_{11} for plane strain compression (-) and uniaxial drawing (--) based on H1.

In Fig. 1 the norm of $\mathbf{D}$ is shown for the simple shear deformation. H1 and H2 stand for the models used in Harren et al. (1989) and Meric et al. (1994), respectively. The curves determined from a calculation with 1000 modified random orientations (Böhlke and Bertram 1998) and two hardening laws indicate that the predictions of both hardening models are almost the same.

The norm of $\mathbf{D}$ is shown in Fig. 2 for the plane strain compression and the drawing deformation. In the former case no saturation of anisotropy is observed in the range $F_{11} \in [0, 10]$, in the latter the magnitude of $\mathbf{D}$ is almost stationary in the range $F_{11} \in [6, 10]$, and so are the components of $\mathbf{C}^V$.

The approximation $\mathbf{C}^{VA}$ of the elasticity tensor $\mathbf{C}^V$, is determined by the condition that $\mathbf{C}^{VA}$ has a certain symmetry group and minimizes the Frobenius norm of $\Delta\mathbf{C} := \mathbf{C}^V - \mathbf{C}^{VA}$. If there is an exact solution $\| \Delta\mathbf{C} \| = 0$ the identification problem is equivalent to that posed and solved by Cowin and Mehrabadi (1987). In order to solve the optimization problem $\| \Delta\mathbf{C} \| \rightarrow \min$ for a given $\mathbf{C}^V$, a direct search polytope algorithm (Gill et al. 1981) has been used. The standard representations of $\mathbf{C}^{VA}$ for different symmetry classes can be easily used, if $\| \Delta\mathbf{C} \|$ is parameterized in form of

$$\| C^V_{ijkl} - Q_{im}Q_{jn}Q_{ko}Q_{lp}\bar{C}^{VA}_{mnop} \| \rightarrow \min,$$

where $\bar{C}^{VA}_{mnop}$ are the components of $\mathbf{C}^{VA}$ with respect to the symmetry axes of the material. The Q_{ij} represent a proper orthogonal matrix describing the rotation from a reference coordinate system to the above mentioned symmetry axes.

In Fig. 3 the norm of $\Delta\mathbf{C}^* := (\mathbf{C}^V - \mathbf{C}^{VA})/\| \mathbf{C} - \mathbf{C}^{VI} \|$ is shown for the plane strain compression deformation and approximations $\mathbf{C}^{VA}$ having the following symmetry groups: (-)= isotropy; (- -)= transverse isotropy $\mathcal{C}_{12}$ and hexagonal systems $\mathcal{C}_{10,11}$; (□)= hexagonal systems $\mathcal{C}_{8,9}$; (-)= cubic system $\mathcal{C}_{6,7}$; (◇)= tetragonal systems $\mathcal{C}_{4,5}$; (o)= rhombic $\mathcal{C}_3$; (+)= monoclinic system $\mathcal{C}_2$ (Gurtin 1972). The approximation with an orthotropic symmetry leads to a significant reduction of $\| \Delta\mathbf{C}^* \|$, which indicates that $\mathbf{C}^V$ possesses an orthotropic symmetry within an acceptable tolerance.

In Fig. 4 the norm of $\Delta \mathbf{C}^*$ is shown for a drawing deformation. In contrast to the rolling deformation, here the approximation with a hexagonal symmetry ($\mathcal{C}_{8,9}$) yields better results than the one with a rhombic, i.e. orthotropic, symmetry.

5. References

Asaro, R.J. and Needleman, A. (1985) Texture development and strain hardening in rate dependent polycrystals. Acta Metall. 33, pp.923–953. Aleksandrov, K. and Aizenberg, L. (1967) *Dokl. Akad. Nauk. SSSR*, 167, pp. 1028–1031.

Bertram, A. and Olschewski, J. (1991) Formulation of anisotropic linear viscoelastic constitutive laws by a projection method. In A. Freed and K. Walker, editors, *High temperature constitutive modelling: Theory and Application*, pp. 129–137. ASME. MD-Vol. 26, AMD-Vol. 121.

Bertram, A. (1999) An Alternative Aproach to Finite Plasticity Based on Material Isomorphisms, *Int. J. Plast.* 15(3), pp. 353–374.

Böhlke, T. and Bertram, A. (1998) Simulation of texture development and induced anisotropy of polycrystals. In S. Alturi and P. O'Donoghue, editors, *Proceedings of ICES'98, Modeling and Simulation Based Engineering*, pp. 1390-1395.

T. Böhlke and A. Bertram (1999) An isotropy condition for discrete sets of cubic single crystals. *Z. Angew. Math. Mech.* 79, S447–448

Bunge, H. (1993) *Texture Analysis in Material Science.* Cuviller Verlag Göttingen.

Cowin, S. and Mehrabadi, M. (1987) On the identification of material symmetry for anisotropic elastic materials. *Q. J. Mech. appl. Math.*, 40, pp. 451–476.

Gill, P.E., Murray, W. and Wright, M. (1981), *Practical Optimization*, Academic Press, New York

Harren, S., Lowe, T., Asaro, R., and Needleman, A. (1989) Analysis of large-strain shear in rate-dependent face-centred cubic polycrystals: Correlation of micro- and macro-mechanics. *Phil. Trans. R. Soc. Lond. A*, 328, pp. 443–500.

Gurtin, M.E. (1972) The Linear Theory of Elasticity. In Encyclopedia of Physics, Vol. VIa/2. Editor C. Truesdell. Springer-Verlag.

Hill, R. (1952) The elastic behaviour of a crystalline aggregate. *Proc. Phys. Soc. Lond.*, A 65, pp. 349–354.

Kocks, U., Tomé, C., and Wenk, H. (1998) *Texture and Anisotropy: Preferred Orientations in Polycrystals and Their Effect on Materials Properties.* Cambridge Univ. Pr.

Leffers, L. (1993). Microstructures, textures and deformation patterns at large strains. In S. Teodosiu, Raphanel, editor, *MECAMAT'91*, pp. 73–86.

Matthies, S. and Humbert, M. (1995) On the principle of a geometric mean of even-rank symmetric tensors for textured polycrystals. *J. Appl. Cryst.*, *28*, pp. 254–266.

Méric, L., Cailletaud, G., and Gaspérini, M. (1994) Calculations of copper bicrystal specimens submitted to tension–compression tests. *Acta metall. mater.*, 42(3), pp. 921–935.

Wu, P., Neale, K., and Van der Giessen, E. (1996) Simulation of the behaviour of fcc polycrystals during reversed torsion. *Int. J. Plast.*, 12(9), pp. 1199–1219.

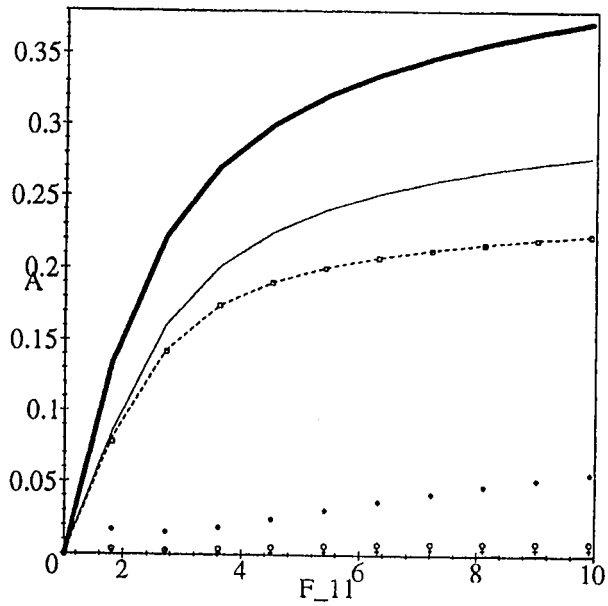

Fig. 3: $A = \| \Delta \mathbf{C}^* \|$ vs F_{11} for plane strain compression.

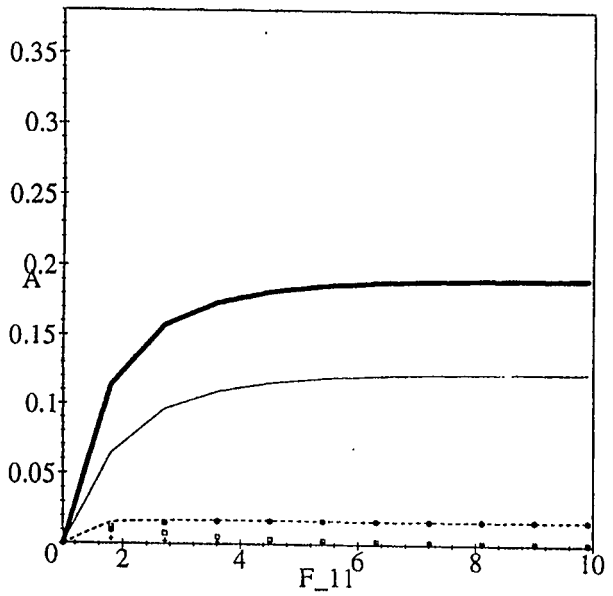

Fig. 4: $A = \| \Delta \mathbf{C}^* \|$ vs F_{11} for drawing.

ICOTOM-12

PROCEEDINGS OF THE TWELFTH INTERNATIONAL CONFERENCE ON TEXTURES OF MATERIALS

Volume 1 of 2 Volumes

McGill University, Montreal, Canada
August 9–13, 1999

Edited by
Jerzy A. Szpunar

Department of Metallurgical Engineering
McGill University
3610 University Street
Montreal, Quebec, Canada H3A 2B2

NRC·CNRC
NRC Research Press
Ottawa 1999